Hydrodynamics of Trickling Flow in Packed Beds: Relative Permeability Concept

Ana Lakota and Janez Levec
Dept. of Chemical Engineering, University of Ljubljana, 1001 Ljubljana, Slovenia

Ruben G. Carbonell
Dept. of Chemical Engineering, North Carolina State University, Raleigh, NC

Liquid holdups and pressure drops for gas and liquid concurrent flow in packed beds were measured experimentally. To calculate the Ergun type constants, pressure drops were also measured for single- (gas)-phase flow through the same packings. These measurements reveal that the Ergun type inertial constant depends on the particle shape. The beds were packed with porous and nonporous spheres, cylinders, extrudates, and Raschig rings. The experimental data were analyzed using the concept of relative permeabilities. The liquid-phase relative permeability correlated well with the reduced liquid saturation in a unique power-law form for all particles independent of their shape. The gas-phase relative permeability as a function of the gas-phase saturation followed the same law, but the exponent depends on the particle shape and gas-phase Reynolds number. Predicted and experimental values for liquid holdups for all particle shapes agreed well with mean relative deviations less than 10%. Predictions of pressure drops for spherical particles, cylinders, and extrudates are at least as accurate as other less rigorous correlations (mean relative errors between 25 and 40%). Pressure drop predictions for Raschig rings are poorer (mean relative deviations of 90%), reflecting in part the variations in pressure drops from experiment to experiment with these particles.

Introduction

A wide variety of process applications utilize the steady, concurrent flow of a gas and a liquid through a packed bed. In reacting systems, this reactor configuration is commonly used for hydrogenation, hydrodesulfurization, denitrogenation, and oxidation reactions and is called a *trickle-bed* reactor. Two of the most significant design and operating parameters of a trickle-bed reactor are the liquid holdup and the two-phase pressure drop. Most of the approaches available to predict the macroscopic liquid holdup and the pressure drop in trickle-bed reactors are fully empirical, with a separate correlation for each one of these parameters. Few attempts have been made to relate the values of the holdup and pressure drop at a given set of operating conditions (Hutton and Leung, 1974; Specchia and Baldi, 1977; Sáez and Carbonell, 1985; Holub et al., 1992). A very complete review of the hydrodynamics of trickle-bed reactors has been recently presented by Attou and Boyer (1999). Very recently, Carbonell (2000) also analyzed the literature on existing continuum models for two-phase flow in packed beds.

One of the most effective and rigorous approaches for two-phase flow analysis is to use spatially averaged equations of motion and continuity in terms of the average velocity and pressure drop in each phase. In this approach, drag force expressions are needed to couple the momentum equations for the gas and liquid. This can be done through the use of relative permeabilities that relate the drag force on a given phase to the local liquid holdup. These relative permeabilities can be measured experimentally. The first information on the nature of the relative permeability functions for two-phase flow in trickle-bed reactors was obtained by Sáez and Carbonell (1985). They developed empirical correlations for relative permeability by analyzing the literature data on pres-

Correspondence concerning this article should be addressed to J. Levec.

sure drop and holdup in trickle-bed reactors. Recently, Attou et al. (1999) developed an analytical fluid-fluid interfacial force model where expressions for the drag force were estimated by considering an idealized liquid- and gas-flow geometry in a single characteristic pore in the porous medium. Even though the approach of Attou et al. (1999) is certainly valid, considerable work needs to be done to compare this theory to experimental results over a wide range of conditions, particle sizes, and particle shapes.

In this work, the applicability of the relative permeability concept is thoroughly tested using porous and nonporous particles of different shapes (spheres, cylinders, extrudates, and Raschig rings). Many of the materials used in this study are representative of the types of catalyst supports and absorber packing materials often used in industry. In order to describe each packing system consistently, two-phase flow pressure drop and holdup measurements were performed after single-phase pressure drop measurements in each packing. Experiments were conducted over a wide range of liquid- and gas-flow rates to better determine the potential effect of gas and liquid Reynolds numbers on relative permeabilities.

Relative Permeability Model: Background

For the case of steady, one-dimensional (1-D), incompressible flow of the gas and liquid through porous media, the volume-averaged momentum equations take the form (Sáez and Carbonell, 1985)

$$\epsilon_\alpha \rho_\alpha v_\alpha \frac{dv_\alpha}{dz} = -\epsilon_\alpha \frac{dP_\alpha}{dz} + \epsilon_\alpha \rho_\alpha g - F_\alpha \tag{1}$$

where $\alpha = \beta, \gamma$, corresponding to liquid and gas phases, respectively. F_α is the drag force per unit volume acting on the α phase. In this equation the velocity and pressure are intrinsic volume averages at a given point in the packed bed, and ϵ_α is the volume fraction of each phase. The continuity equations for liquid and gas phases for this case take the simple form

$$L = \epsilon_\beta \rho_\beta v_\beta$$

$$G = \epsilon_\gamma \rho_\gamma v_\gamma \tag{2}$$

L and G are here the liquid and gas mass fluxes, respectively.

For the case of 1-D flow, the average velocities and liquid holdups are essentially independent of position along the bed, so inertial terms in the momentum equations are negligible. The pressure gradients in this case in the liquid and gas phases are equal since the liquid saturation is a constant along the column. Since the liquid and gas volume fractions sum up to total bed void fraction ϵ, the momentum equations for the liquid and gas can be used to solve for the pressure drop and liquid holdup in the column. This requires constitutive equations for the drag force expressions.

Sáez and Carbonell (1985) introduced the relative permeability concept to come up with expressions for the drag force per unit volume in each phase. The relative permeability is defined as the ratio between the drag force per unit volume under one-phase flow conditions, to the drag force per unit volume under single-phase flow conditions at the same superficial velocity of a given phase; thus

$$k_\alpha = \frac{(F_\alpha/\epsilon_\alpha)^0}{(F_\alpha/\epsilon_\alpha)} \tag{3}$$

For example, using an Ergun-type equation for the single-phase pressure drop, the two-phase flow pressure drop can be written in the form

$$\frac{F_\alpha}{\epsilon_\alpha} = \frac{1}{k_\alpha(S_\alpha)}\left[A\frac{Re_\alpha}{Ga_\alpha} + B\frac{Re_\alpha^2}{Ga_\alpha}\right]\rho_\alpha g \tag{4}$$

The Ergun equation here has been made dimensionless with the Reynolds and Galileo numbers. This recognizes the importance of gravitational forces in the liquid flow.

The concept of relative permeability has been used to correlate two-phase flow drag forces in a porous medium, primarily in underground flows. The relative permeability takes into account the blockage of flow in a pore as a result of the presence of a second phase. As a result, the relative permeability for a given phase is considered a function only of the fraction of the pore volume occupied by that phase. This ratio is referred to as the saturation for each phase

$$S_\alpha = \frac{\epsilon_\alpha}{\epsilon} \tag{5}$$

The relative permeability corrects the expression for the drag force under single-phase flow conditions to account for the flow of two phases. As a result, the definition of the relative permeability demands that as the saturation of a given phase approaches one, the relative permeability for that phase approaches one to recover the single-phase flow drag force expression

$$k_\alpha \to 1 \quad \text{as} \quad S_\alpha \to 1 \tag{6}$$

Once the drag force expressions for the gas and liquid phases are known, the gas-phase equation of motion can be used to compute the pressure drop, which in dimensionless form can be written as

$$\Psi_\gamma = \frac{1}{\rho_\gamma g}\left[-\frac{\Delta(P_\gamma - \rho_\gamma g Z)}{Z}\right] = \frac{F_\gamma}{\epsilon_\gamma} = \frac{1}{k_\gamma}\left[A\frac{Re_\gamma}{Ga_\gamma} + B\frac{Re_\gamma^2}{Ga_\gamma}\right]\rho_\gamma g \tag{7}$$

The momentum equations for the gas and liquid phases can be subtracted from each other, assuming the liquid density is much greater than the gas-phase density, to obtain an equation that can be solved for the liquid holdup

$$\frac{1}{k_\beta}\left[A\frac{Re_\beta}{Ga_\beta} + B\frac{Re_\beta^2}{Ga_\beta}\right] - \frac{1}{k_\gamma}\left[A\frac{Re_\gamma}{Ga_\gamma} + B\frac{Re_\gamma^2}{Ga_\gamma}\right]\frac{\rho_\gamma}{\rho_\beta} = 1 \tag{8}$$

Recall that both k_β and k_γ are functions only of the saturation S_β and $S_\gamma = 1 - S_\beta$.

Given the particle diameter, and the gas and liquid mass fluxes, it is possible to calculate the Reynolds and Galileo numbers for both phases. Knowing the relative permeability as a function of saturation for the gas and liquid phases, Eq. 8 can be solved for the liquid holdup. Equation 7 can then be used to compute the two-phase flow pressure drop.

Sáez and Carbonell (1985) obtained empirical expressions for the gas- and liquid-phase relative permeabilities by analyzing two-phase holdup and pressure drop data available at that time. These expressions were written as a function of the gas saturation and liquid reduced phase saturation, respectively

$$k_\beta = \delta_\beta^m; \quad m = 2.43$$

$$k_\gamma = S_\gamma^n; \quad n = 4.8 \tag{9}$$

where the reduced liquid-phase saturation δ_β is defined by

$$\delta_\beta = \frac{\epsilon_\beta - \epsilon_\beta^0}{\epsilon - \epsilon_\beta^0} \tag{10}$$

In Eq. 10, ϵ_β^0 is the residual liquid holdup that remains upon draining the column, a quantity estimated and measured by several previous investigators (Carbonell, 2000). For the decreasing liquid-flow rate mode at a stagnant gas phase, Levec et al. (1986) later showed that the liquid-phase relative permeability was best represented with the following expression

$$k_\beta = \begin{cases} \delta_\beta^{2.9}; & \delta_\beta \geq 0.2 \\ 0.25\delta_\beta^{2.9}; & \delta_\beta < 0.2 \end{cases} \tag{11}$$

On the basis of experimental observations, they also found that the gas-phase relative permeability might depend on the gas-phase Reynolds number and probably on the particle diameter. They reported exponents in the range from 3.6 to 7.5 in a power fit of k_γ vs. S_γ for spherical nonporous particles. In all these calculations the constants A and B in the modified Ergun equation were set equal to 180 and 1.8, respectively, as recommended by McDonald et al. (1979). Even though Raschig rings and cylinders were included in the data base for the development of Eq. 9, most of the information available was for spherical particles.

Experimental Apparatus and Procedure

The experimental system and procedure used in this study is previously described in detail by Levec et al. (1986). The column had dimensions of 17.2 cm ID, and 130 cm of total packing length. The flow distributor had 550 capillary tubes at 0.6 cm pitch with 0.09 cm ID and 3.0 cm length, through which water was introduced into the column. The capillaries were held between two Pertinax plates that were 2.5 cm apart. The bottom plate had circular holes around the capillaries. The holes were slightly larger in diameter than the outer diameter of the capillary tubes. The air was introduced into the chamber formed between the plates, and it exited the distributor through these holes. The top of the packing was 0.5 cm below the distributor. The dynamic liquid holdup was measured by weighing the column during the operation by means of a strain gauge (Hottinger Baldwin Messtechnik, Germany) with a sensitivity of 360 V/kg, allowing the detection of a 5 g weight difference from a total dry column weight of 80 kg. Pressure drops were measured by two pressure transducers with a range of 0−0.05 bar and 0−0.2 bar, respectively (Hottinger Baldwin Messtechnik, Germany). The structural properties of the packing materials are summarized in Table 1, while the operating conditions for the column are given in Table 2.

In all experiments, the column was carefully preflooded and then allowed to drain for about 30 min; at this point, a residual amount of liquid (static holdup) remained in the bed and was determined by the difference in weight between the dry and wet column. In the two-phase experiments the column was operated first at very high liquid- and gas-flow rates

Table 1. Properties of the Packing Material

Particle Shape	Actual Dimension (mm)	Equiv. Dia. (mm)	Bed Porosity	Static Holdup
Nonporous spheres *Glass*	3.0	3.0	0.375	0.022
Nonporous spheres *Glass*	6.0	6.0	0.385	0.023
Porpus spheres *Alumina*	3.7	3.7	0.39	0.021
Porous spheres *Silica*	5.5	5.5	0.39	0.022
Porous cylinders *Zinc-copper oxide/alumina*	4.5×4.5	4.5	0.42	0.022
Porous cylinders *Iron-molybdate catalyst*	3.9×3.2	3.6	0.415	0.037
Porous extrudates *Zinc aluminate spinel*	1.3×5.0*	1.8	0.46	0.028
Rashing rings *Ceramics*	8.5×5.5	4.1	0.58	0.028

*Average length.

Table 2. Operating Conditions

Column inner diameter	17.2 cm
Total packing length	122 cm
Temperature	21 ± 1°C
Mass-flow rate range:	
Air	$0-0.37$ kg/m$^2 \cdot$s
Water	$0.06-25.1$ kg/m$^2 \cdot$s

(pulsing flow) in order to assure complete wetting of the bed. This led to highly reproducible measurements. Pressure drops and liquid holdups were measured simultaneously during both modes of operation (increasing and decreasing liquid flow rates), but only the results obtained in the decreasing mode are reported here. In separate experiments the "end effects" contributed by the supporting stainless steel screen at the column bottom on both the liquid holdup and pressure drop were determined. However, the results presented herein are the averages of measurements obtained from at least three (re)packed beds. Thus, over 600 data points were used for the evaluation of permeabilities.

Results and Discussion

Single-phase pressure drop

The experimental pressure drops obtained under the single-phase flow conditions are plotted in Figure 1 as a function of the gas-phase Reynolds number. From this figure, one can see that the Ergun equation with $A = 150$ and $B = 1.75$ predicts the pressure drop accurately only in the beds packed with spherical particles (within 10.5%), but fails in the case of nonspherical particles. The Ergun equation (1952) underestimates the single-phase pressure drop up to 30% in the case of cylinders and more than 60% in beds packed with Raschig rings and extrudates. The Ergun type equation with the constants recommended by McDonald et al. (1979) also disagrees with the experimental data (Table 3). For spherical particles, the constant B was allowed to be 1.8 and for nonspherical porous particles 4. In this case the predicted pressure drops are slightly overestimated for spherical particles and cylinders, but they are still about 20% to 30% lower than the experimental for Raschig rings and extrudates. The results in Figure 1 indicate that the values of the constants A and B in the Ergun type equation depend on the structure of the porous matrix, and they can vary appreciably. An application of a data fit optimization algorithm (Marquardt, 1963) on both parameters over the entire range of operating conditions for each particle size and shape resulted in a variation in the value of A from 118 to 381 and B from 1.71 up to 6.65. For spheres, this approach did not improve the prediction of the pressure drop significantly (the mean relative error e_y dropped less than 2%). The mean relative error for other particles was between 2.06% and 13.6%. While analyzing the experimental single-phase pressure drop data, it appeared that the viscous term in the Ergun-type equation is rather independent of the particle shape, in contrast with the inertial term. Therefore, we decided to let the value of A be 150, whereas the values of B for nonspherical particle shapes were optimized as previously mentioned. With this approach, the mean relative error is still within 15.3%. The statistical analyses of the pressure drop fits for all particles used in this study are presented in Table 3.

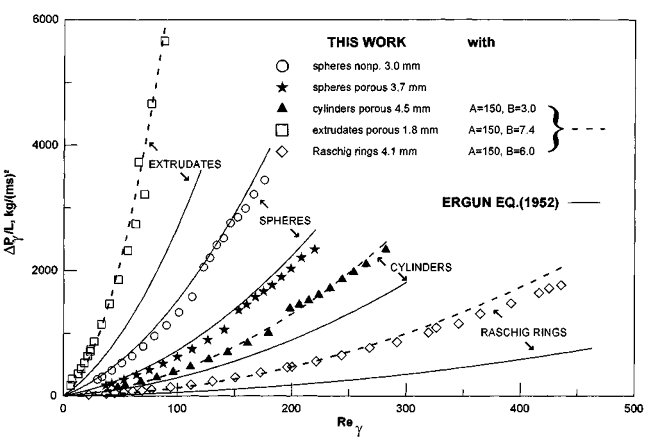

Figure 1. Experimental single-phase pressure drops vs. the Ergun-type equations.

Two-phase flow operation

Gas-Phase Relative Permeability. The pressure drop and the liquid holdup data were taken in the decreasing liquid flow rate operation mode, that is, from the upper branch of the hysteresis loop in the low interaction regime (Levec et al.,1986). The gas-phase relative permeabilities were calculated from the relation

$$k_\gamma = \frac{\psi_\gamma^0}{\psi_\gamma} \tag{12}$$

Table 3. Single-Phase Pressure Drop Measurements

		Ergun (1952) $A = 150$ $B = 1.75$	McDonald et al. (1979) $A = 180$		This Work Fit				
					Two-Parameter			One-Parameter $A = 150$	
Particles	d_e (mm)	e_y (%)	B	e_y (%)	A	B	e_y (%)	B	e_y (%)
Nonporous spheres	3.0	8.15	1.8	17.26	127	1.7	7.34		
	6.0	5.30	1.8	11.47	160	1.6	4.26		
Porous spheres	3.7	10.55	1.8	18.77	127	5.4	10.5		
	5.5	5.52	1.8	7.92	118	1.95	3.54		
Porous cylinders	4.5	31.4	4	28.6	187	2.8	3.19	3.0	4.38
Porous extrudates	1.8	51.24	4	26.8	170	6.65	13.6	7.4	15.3
Raschig rings	4.1	62.2	4	28.7	381	4.7	2.06	6.0	11.7

Table 4. Dimensionless Variables

Particles	d_e (mm)	$Ga_{\gamma*}$	$Re_{\gamma*}$	Ga_β	Re_β
Spheres	3.0	249	3.67– 97.4	43,220	0.20–157.9
Spheres	6.0	2,071	14.75–193.2	359,200	0.80–116.5
Spheres	3.7	524	4.59–107.1	90,867	1.20– 84.6
Spheres	5.5	1,636	6.78–102.2	283,770	1.80– 89.3
Cylinders	4.5	1,352	29.30–119.1	235,015	0.39–162.3
Cylinders	3.6	651	23.53– 96.1	113,130	0.31–128.7
Extrudates	1.8	141	0.51– 63.2	24,485	0.16– 69.7
Raschig rings	4.1	6,888	29.30– 96.1	1,279,215	0.49–205.6

*Calculated at 1 bar.

where ψ_γ^0 and ψ_γ are the dimensionless pressure drops measured under single- (gas-phase) and two-phase flow conditions, respectively, at the same gas superficial velocity. In this experimental study a wide range of values of the dimensionless variables were used (Table 4). The gas-phase Galileo number Ga_γ was in the range of 141 to nearly 7,000, and the gas-phase Reynolds number Re_γ varied from 0.51 to 193. The liquid-phase Reynolds number Re_β took the values from 0.16 to about 200 and the liquid-phase Galileo number Ga_β spread over three decades, that is, from 24,485 to more than one million. In Figure 2 typical results of the experimentally determined gas-phase relative permeabilities as a function of the gas saturation are shown for spherical particles (6.0 mm nonporous spheres) and nonspherical particles (porous extrudates). It is clear that this relation cannot be represented by a single curve. At constant liquid Reynolds number, the data lie nearly vertically in these graphs, indicating that there is no direct effect of the liquid flow rate on k_γ but through the liquid holdup (see Figure 3). Consequently, for each particle size and shape, k_γ was correlated as a power-law function of the gas-phase Reynolds number (Re_γ) of the same form as

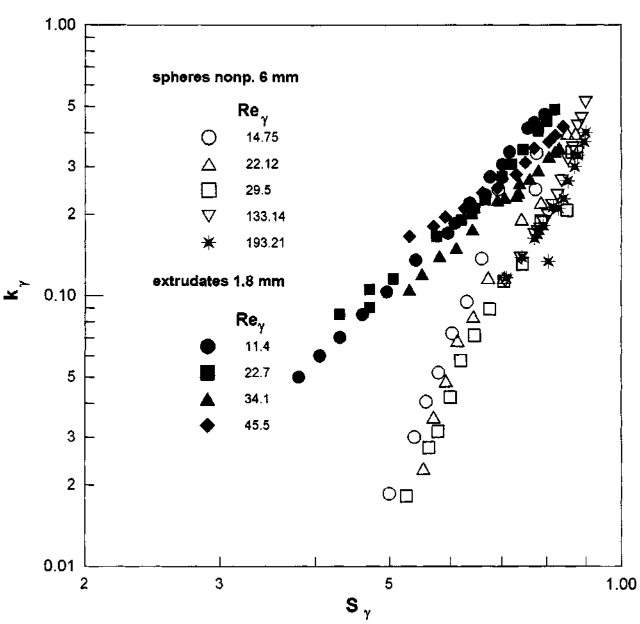

Figure 2. Experimental gas-phase relative permeabilities as a function of gas-phase Reynolds number.

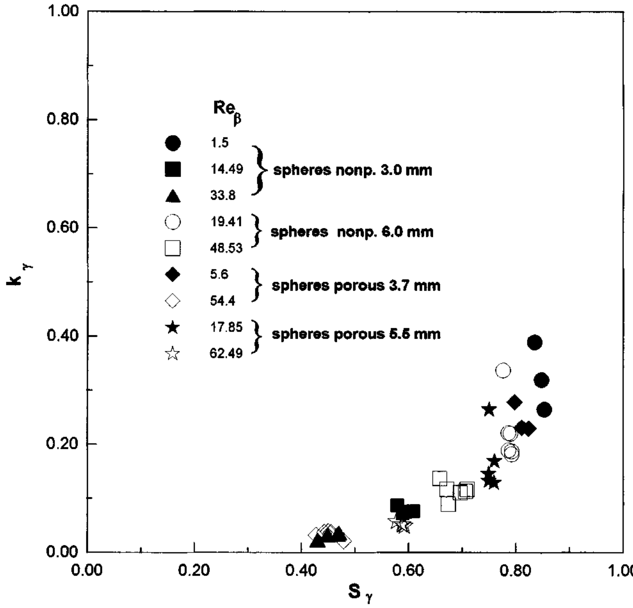

Figure 3. Experimental gas-phase relative permeabilities, with liquid-phase Reynolds number as parameter.

Eq. 9. Contrary to the previous results of Sáez and Carbonell (1985) and of Levec et al. (1986), who did not have the benefit of a large amount of data to analyze on gas-phase relative permeabilities, it was found that the exponent n is practically independent of the particle size, but is strongly affected by the particle shape and the gas-phase Reynolds number. This dependence is depicted in Figure 4 and is correlated by an expression proposed by Lakota (1991)

$$n = \chi + 0.0478 \times \left(Re_\gamma \right)^{0.774} \tag{13}$$

where the constant χ depends on the particle shape (Table 5). Thus, Eq. 13 can be used to estimate the exponent n for a given particle geometry when the gas-phase Reynolds number is provided.

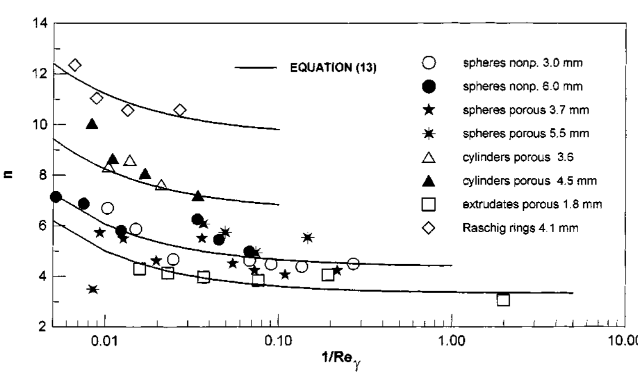

Figure 4. Gas-phase relative permeability exponent as a function of gas-phase Reynolds number.

Table 5. Dimensionless Constant χ in Eq. 13

Particles	χ
Spheres	4.37
Cylinders	6.54
Extrudates	3.31
Raschig rings	9.52

Liquid-Phase Relative Permeability. In the prior work (Sáez and Carbonell, 1985; Levec et al., 1986), the liquid-phase relative permeabilities were measured under stagnant gas-phase conditions. They were obtained in this work from the two-phase flow experiments by using Eq. 8 with the second term on the lefthand side of the equation replaced by the experimentally measured two-phase pressure drops, namely

$$k_\beta = \frac{\left[150\frac{Re_\beta}{Ga_\beta} + B\frac{Re_\beta^2}{Ga_\beta}\right]}{1+(\psi_\gamma)_{\exp}\frac{\rho_\gamma}{\rho_\beta}} \tag{14}$$

where the constant B for a given particle shape was taken from Table 3. Lakota (1991) showed that the liquid relative permeability was a unique function of the liquid reduced saturation. An expression, similar to Eq. 11 (Levec et al., 1986), was found to be valid for all particles used in the present experimental study, regardless of size, roughness and shape

$$k_\beta = \begin{cases} \delta_\beta^{2.92}; & \delta_\beta \geq 0.3 \\ 0.40\,\delta_\beta^{2.12}; & \delta_\beta < 0.3 \end{cases} \tag{15}$$

This correlation is shown in Figure 5. The results imply that in the trickle-flow regime the flowing gas phase does not contribute significantly to the drag forces between the fluid phases.

Prediction of Liquid Holdup and Two-Phase Pressure Drop. Knowing the liquid-phase relative permeability as a function of the liquid-phase reduced saturation, and the gas-phase relative permeability as a function of the gas-phase saturation,

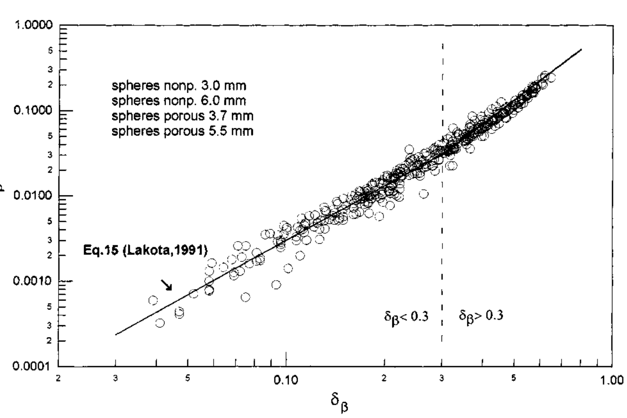

Figure 5. Liquid relative permeabilities as a function of reduced liquid saturation: spherical particles.

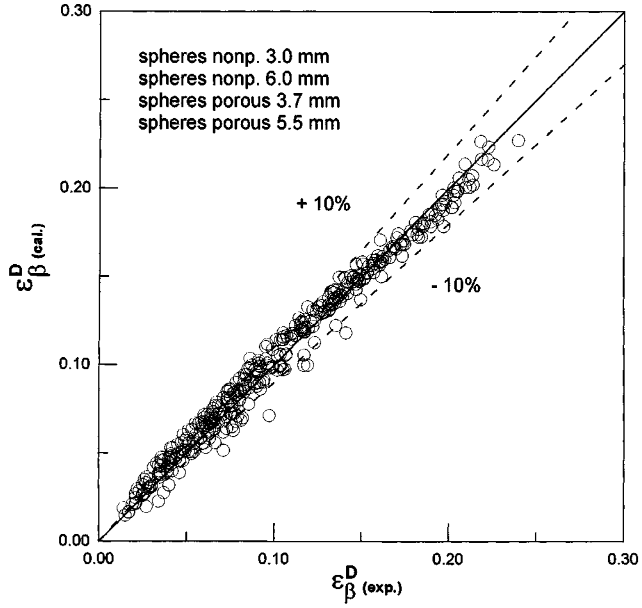

Figure 6. Predicted vs. experimental liquid holdups: spherical particles.

one can write Eq. 8 in the following form

$$\frac{1}{f}\times\left(\frac{\epsilon-\epsilon_\beta^0}{\epsilon_\beta-\epsilon_\beta^0}\right)^m\left[150\frac{Re_\beta}{Ga_\beta}+B\frac{Re_\beta^2}{Ga_\beta}\right]-\left(\frac{\epsilon}{\epsilon-\epsilon_\beta}\right)^n \times\left[150\frac{Re_\beta}{Ga_\beta}+B\frac{Re_\gamma^2}{Ga_\beta}\right]\frac{\rho_\gamma}{\rho_\beta}=1 \tag{16}$$

and solve it for the only unknown, the liquid holdup ϵ_β. In calculating the liquid holdup, the value of m is either 2.92 (when factor f equals 1) for $\delta_\beta \geq 0.3$, or 2.12 for $\delta_\beta < 0.3$ (in this case factor f is 0.40). The constant B in the above equation depends upon the particle shape (Table 3). The appropriate value of n can be estimated by means of Eq. 13. Once the liquid holdup is determined, Eq. 7 can be written in the form

$$\psi_\gamma = \left(\frac{\epsilon}{\epsilon-\epsilon_\beta}\right)^n\left[150\frac{Re_\gamma}{Ga_\gamma}+B\frac{Re_\gamma^2}{Ga_\gamma}\right] \tag{17}$$

and used to compute the two-phase pressure drop.

The calculated values of the liquid holdups for spherical and nonspherical particles are compared to the experimental ones in Figures 6 and 7, respectively, whereas Figures 8 and 9 show the predictions of the two-phase pressure drops. For each particle shape, the mean absolute relative error (e_y), as well as the mean relative deviation (σ) in the prediction of the both hydrodynamic parameters, are presented in Table 6.

As one can see, the majority of liquid holdup data points lies within the confidence interval of $\pm 10\%$, whereas this is not the case with the pressure drop data. For example, for the liquid holdup e_y is 7.65% for spheres, 10.6% for cylinders, 11.9% for extrudates, and 9.1% for Raschig rings. On

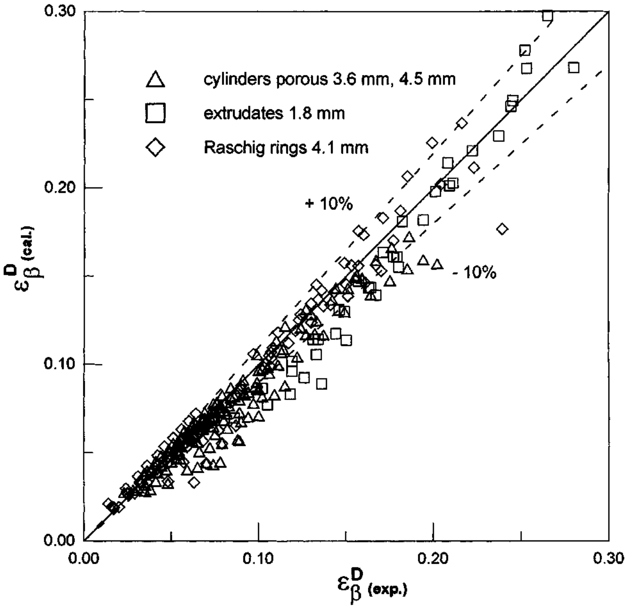

Figure 7. Predicted vs. experimental liquid holdups: nonspherical particles.

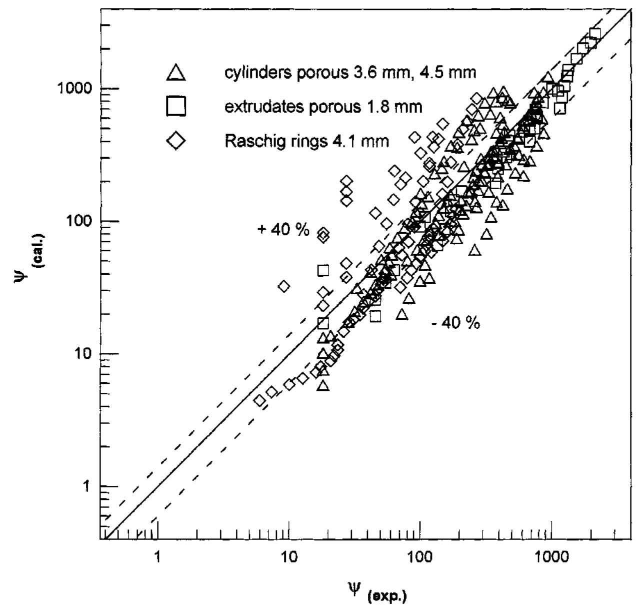

Figure 9. Predicted vs. experimental two-phase pressure drops: nonspherical particles.

the other hand, the pressure drop data correlate with a mean relative error of 29.8% for spheres, 41.5% for cylinders, 25.4% for extrudates, and 91.3% for Raschig rings. The results of the correlations for spheres, cylinders, and extrudates are as good as those found with any of the empirical correlations available in the literature. Given the variability in the experimental data from experiment to experiment with the Raschig rings, the larger mean relative error and mean relative deviations of these packing materials are not that surprising. The analysis of the experimental results using the relative permeability concept validate this approach for the correlation and calculation of two-phase flow behavior in packed beds, especially for spheres and cylinders as packing materials.

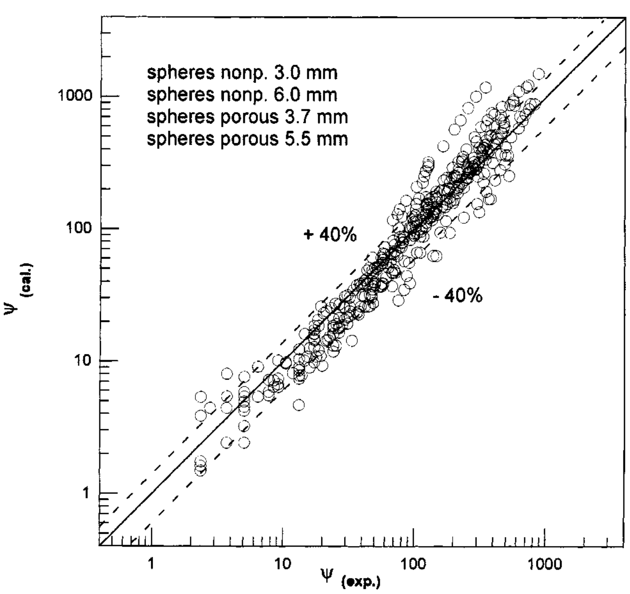

Figure 8. Predicted vs. experimental two-phase pressure drops: spherical particles.

Conclusions

The relation between the liquid relative permeability and the reduced liquid saturation is expressed by a unique power-law function, where the exponent does not depend on the particle shape. The correlation for predicting the liquid holdups, which uses the Ergun type constants obtained under the single-phase flow conditions, provides excellent results for beds packed either with spherical or nonspherical particles. It was found that the relation between the gas-phase relative permeability and the gas-phase saturation also follows a one-parameter exponential function, but the exponent depends on the particle shape, as well as on the gas-phase Reynolds number. Although the experimentally evaluated Ergun type inertial constants were used, the predictions are

Table 6. Liquid Holdups and Two-Phase Pressure Drops Prediction (Statistics)

Particles	No. of Exp. Points	Dynamic Liquid Holdup (ϵ_β^D)		Pressure Drop (ψ)	
		e_y (%)	σ (%)	e_y (%)	σ (%)
Spheres (d_e = 3.0; 3.7; 5.5; 6.0 mm)	365	7.65	7.8	29.8	34.4
Cylinders (d_e = 3.6; 4.5 mm)	132	10.6	9.6	41.5	50.7
Extrudates (d_e = 1.8 mm)	37	11.9	8.8	25.4	23.0
Raschig rings (d_e = 4.1 mm)	91	9.1	9.6	91.3	50.1

not as good as for the liquid holdups. This is true for all other correlation approaches in the literature due to the larger variations found in measured pressure drops. While a large majority of the pressure drop data points for spherical particles, cylinders and extrudates are found within the confidence limits of $\pm 40\%$, a large portion of the data for Raschig rings are found outside these limits. This disagreement is due to the variability in pressure drop data with the Raschig rings.

Acknowledgment

The authors are thankful for the financial support provided by the Slovenian Ministry of Science and Technology through grant P0-0510-0103.

Notation

A = constant in the viscous term of the Ergun type equation
B = constant in the inertial term of the Ergun type equation
d_e = equivalent particle diameter, m $(=6V_p/S_p)$
F_α = drag force on the α phase per unit volume, kg/m$^2\cdot$s^2
G = gas mass flux, kg/m$^2\cdot$s
Ga_α = Galileo number of the α phase $=\{(\rho_\alpha^2 g d_e^3 \epsilon^3)/[\mu_\alpha^2(1-\epsilon)^3]\}$
k_α = relative permeability of the α phase
L = liquid mass flux, kg/m$^2\cdot$s
m = exponent in the liquid phase relative permeability relation
n = exponent in the gas phase relative permeability relation
ΔP_α = pressure drop of the α phase, kg$\cdot$m$^{-1}\cdot$s^{-2}
Re_α = Reynolds number of the α phase $[=(\rho_\alpha u_\alpha/\mu_\alpha \epsilon) d_e(\epsilon/1-\epsilon)]$
S_p = particle surface area, m
S_α = saturation of the α phase, $(=\epsilon_\alpha/\epsilon)$
u_α = superficial velocity of the α phase, m$\cdot$s^{-1}
v_α = intrinsic velocity of the α phase, $(=u_\alpha/\epsilon)$
V_p = particle volume, m^3
Z = packing length, m

Greek letters

δ_β = reduced saturation of the liquid phase
ϵ_β^D = dynamic liquid holdup
ϵ = bed porosity
ϵ_β = total liquid holdup per unit volume of the bed
ϵ_β^0 = static liquid holdup
μ_α = viscosity of the α phase, kg$\cdot$m$^{-1}\cdot$s^{-1}
ρ_α = density of the α phase, kg$\cdot$m^{-3}
χ = dimensionless constant, Eq. 13
ψ_α = dimensionless two-phase pressure drop

Subscripts

α = gas and/or liquid phase
β = liquid phase
γ = gas phase

Literature Cited

Attou, A., and C. Boyer, "Revue des Aspects Hydrodynamiques des Réacteurs Catalytiques Gaz-Liquide-Solide á Lit Fixe Arrosé," *Oil & Gas Sci. and Technol.—Revue de l'IFP*, **54**, 29 (1999).

Attou, A., C. Boyer, and G. Ferschnider, "Modelling of the Hydrodynamics of the Cocurrent Gas-Liquid Trickle Flow Through a Trickle Bed Reactor," *Chem. Eng. Sci.*, **54**, 785 (1999).

Carbonell, R. G., "Multiphase Flow Models in Packed Beds," *Oil and Gas Sci. and Technol.*, **55**, 417 (2000).

Holub, R. A., M. P. Dudukovic, and P. A. Ramachandran, "A Phenomenological Model for Pressure Drop, Liquid Holdup, and Flow Regime Transition in Gas-Liquid Trickle Flow," *Chem. Eng. Sci.*, **47**, 2343 (1992).

Hutton, B. E. T., and L. S. Leung, "Cocurrent Gas-Liquid Flow in Packed Columns," *Chem. Eng. Sci.*, **29**, 1681 (1974).

Lakota, A., "Hydrodynamic and Mass Transfer Characteristics in Trickle Bed Reactor," PhD Thesis, Univ. of Ljubljana, Slovenia (1991).

Levec, J., A. E. Sáez, and R. G. Carbonell, "The Hydrodynamics of Trickling Flow in Packed Beds: II. Experimental Observations," *AIChE J.*, **32**, 369 (1986).

Marquardt, D. W., "An Algorithm for Least-Squares Estimation of Nonlinear Parameters," *J. Soc. Indust. Appl. Math.*, **11**, 431 (1963).

McDonald, I. F., M. S. El-Sayed, K. Mow, and F. A. L. Dullien, "Flow Through Porous Media—the Ergun Equation Revisited," *Ind. Eng. Chem. Fund.*, **18**, 199 (1979).

Sáez, A. E., and R. G. Carbonell, "Hydrodynamic Parameters for Gas-Liquid Cocurrent Flow in Packed Beds," *AIChE J.*, **31**, 52 (1985).

Specchia, V., and G. Baldi, "Pressure Drop and Liquid Holdup for Two-Phase Concurrent Flow in Packed Beds," *Chem. Eng. Sci.*, **32**, 515 (1977).

Manuscript received Mar. 26, 2001, and revision received Sept. 5, 2001.